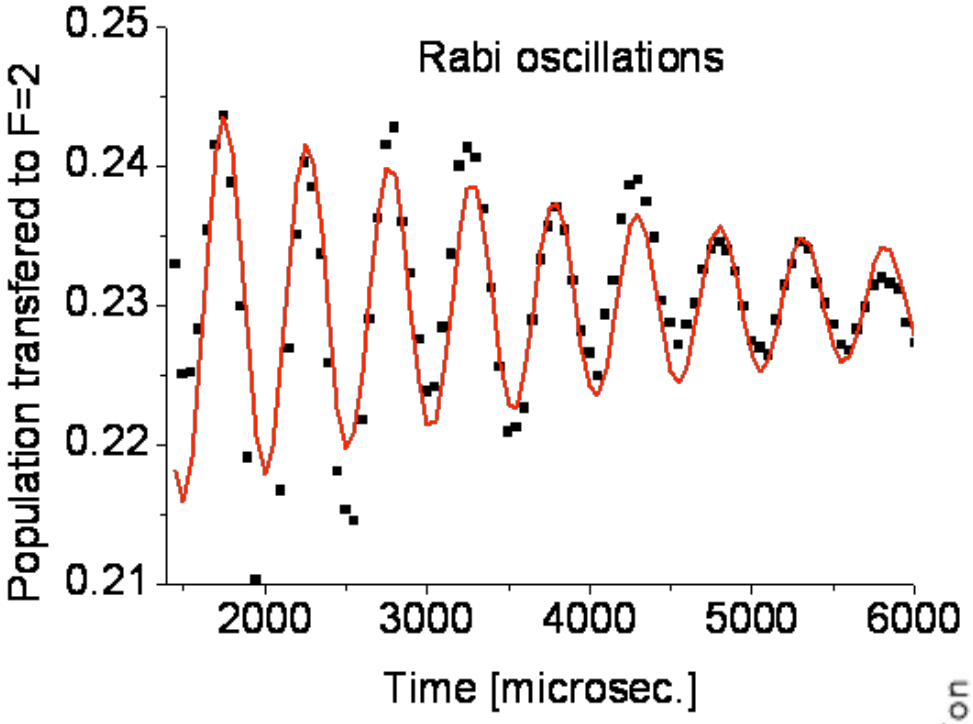
Rabi oscillations
Population transfered to F=2
0.25
0.24
0.23
0.22
0.21
2000
3000
4000
5000
6000
Time [microsec.]

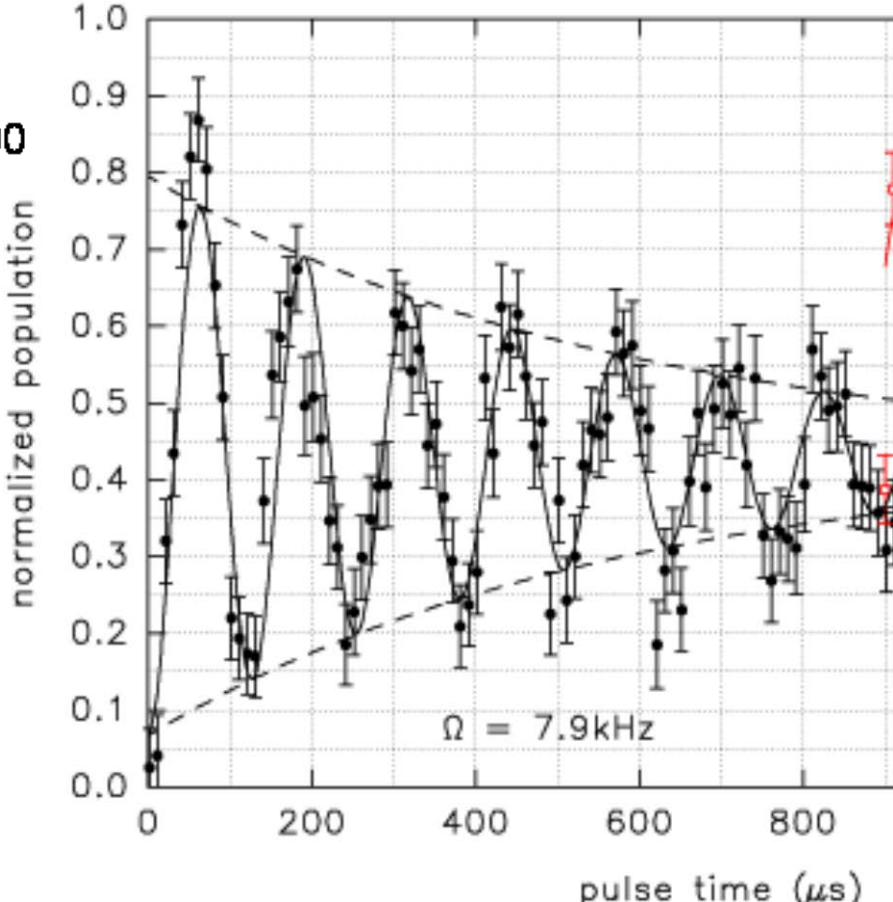
normalized population
1.0
0.9
0.8
0.7
0.6
0.5
0.4
0.3
0.2
0.1
0.0
Ω = 7.9kHz
0
200
400
600
800
pulse time (μs)

On-Demand Single Photons with High Extraction Efficiency and Near-Unity Indistinguishability from a Resonantly Driven Quantum Dot in a Micropillar

Xing Ding,[1,2,3] Yu He,[1,2,3] Z.-C. Duan,[1,2,3] Niels Gregersen,[4] M.-C. Chen,[1,2,3] S. Unsleber,[5] S. Maier,[5] Christian Schneider,[5] Martin Kamp,[5] Sven Höfling,[1,5,6] Chao-Yang Lu,[1,2,3,*] and Jian-Wei Pan[1,2,3,†]

Scalable photonic quantum technologies require on-demand single-photon sources with *simultaneously* high levels of purity, indistinguishability, and efficiency. These key features, however, have only been demonstrated separately in previous experiments. Here, by *s*-shell pulsed resonant excitation of a Purcell-enhanced quantum dot-micropillar system, we deterministically generate resonance fluorescence single photons which, at π pulse excitation, have an extraction efficiency of 66%, single-photon purity of 99.1%, and photon indistinguishability of 98.5%. Such a single-photon source for the first time combines the features of high efficiency and near-perfect levels of purity and indistinguishabilty, and thus opens the way to multiphoton experiments with semiconductor quantum dots.

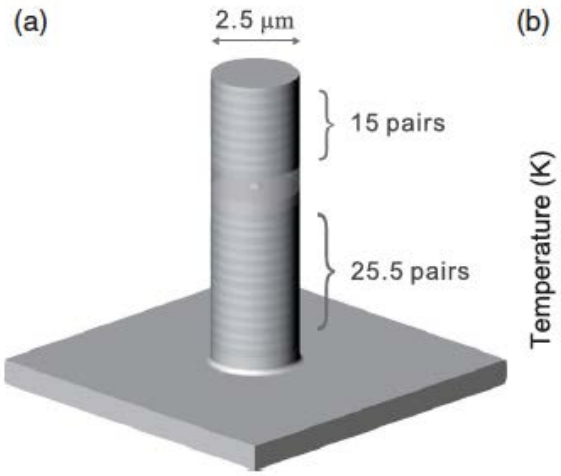

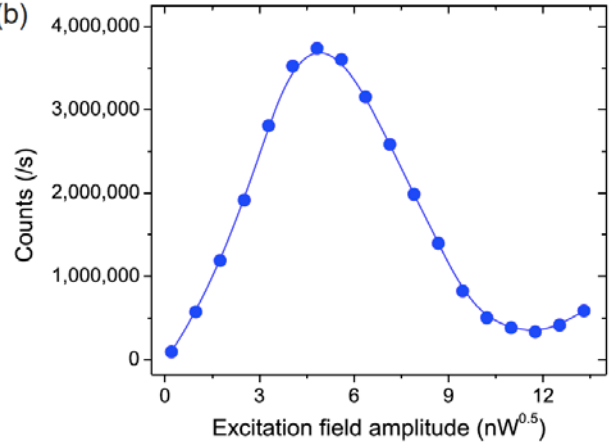

Rabi oscillation (resonance fluorescence)
→ peak excitation for 24 nW laser power

How does a pi-pulse de-excite an atom more quickly than spontaneous decay?

The Zeno's paradox in quantum theory

Misra, B.; Sudarshan, E. C. G.

Journal of Mathematical Physics 18, pp. 756-763 (1977).

Time evolution of unstable quantum states and resolution of Zeno's paradox

Chiu, Sudarshan and Misra, Phys Rev. D **16**, 520 (1977)

What are Quantum Jumps? Richard J Cook, Physica Scripta **T21**, 49 (1988)

PHYSICAL REVIEW A **VOLUME 41, NUMBER 5** **1 MARCH 1990**

Quantum Zeno effect

Wayne M. Itano, D. J. Heinzen, J. J. Bollinger, and D. J. Wineland

Time and Frequency Division, National Institute of Standards and Technology, Boulder, Colorado 80303

(Received 12 October 1989)

The quantum Zeno effect is the inhibition of transitions between quantum states by frequent measurements of the state. The inhibition arises because the measurement causes a collapse (reduction) of the wave function. If the time between measurements is short enough, the wave function usually collapses back to the initial state. We have observed this effect in an rf transition between two $^9Be^+$ ground-state hyperfine levels. The ions were confined in a Penning trap and laser cooled. Short pulses of light, applied at the same time as the rf field, made the measurements. If an ion was in one state, it scattered a few photons; if it was in the other, it scattered no photons. In the latter case the wave-function collapse was due to a null measurement. Good agreement was found with calculations.

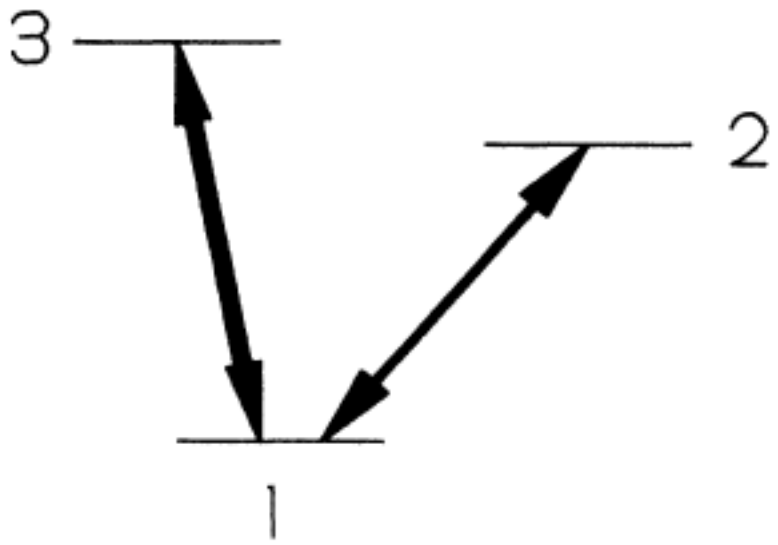

FIG. 1. Energy-level diagram for Cook's proposed demonstration of the quantum Zeno effect.

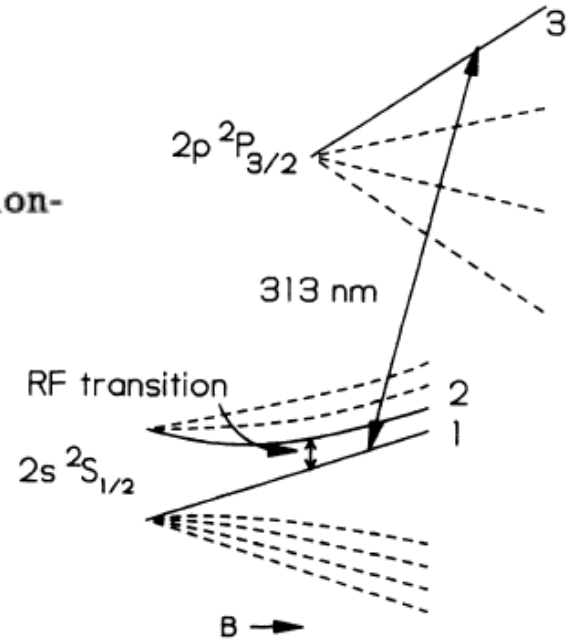

FIG. 2. Diagram of the energy levels of $^9Be^+$ in a magnetic field B. The states labeled 1, 2, and 3 correspond to those in Fig. 1 .

TABLE I. Predicted and observed values of the $1 \rightarrow 2$ and $2 \rightarrow 1$ transition probabilities for different values of the number of measurement pulses n. The uncertainties of the observed transition probabilities are about 0.02. The second column shows the transition probabilities that result from a simplified calculation, in which the measurement pulses are assumed to have zero duration and in which optical pumping is neglected.

		$1 \rightarrow 2$ transition		$2 \rightarrow 1$ transition	
n	$\frac{1}{2}[1-\cos^n(\pi/n)]$	Predicted	Observed	Predicted	Observed
1	1.0000	0.995	0.995	0.999	0.998
2	0.5000	0.497	0.500	0.501	0.496
4	0.3750	0.351	0.335	0.365	0.363
8	0.2346	0.201	0.194	0.217	0.209
16	0.1334	0.095	0.103	0.118	0.106
32	0.0716	0.034	0.013	0.073	0.061
64	0.0371	0.006	−0.006	0.080	0.075

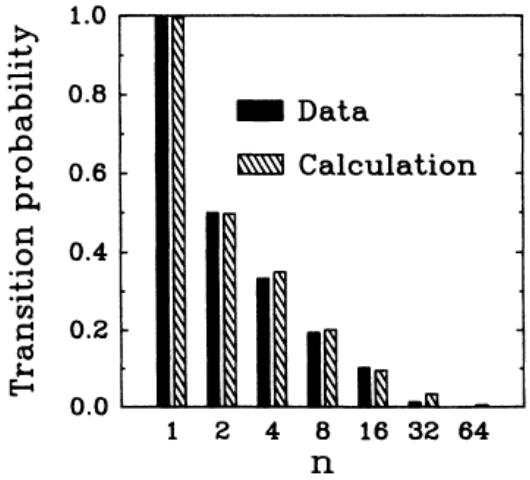

FIG. 3. Graph of the experimental and calculated $1 \rightarrow 2$ transition probabilities as a function of the number of measurement pulses n. The decrease of the transition probabilities with increasing n demonstrates the quantum Zeno effect.

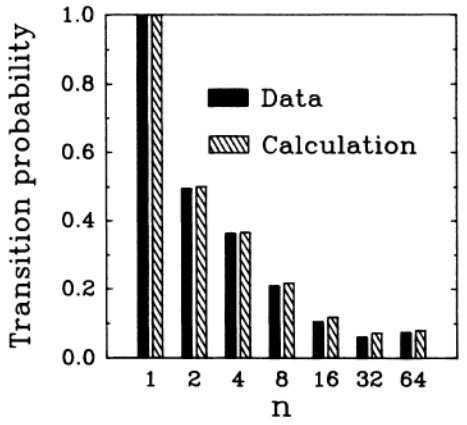

FIG. 4. Graph of the experimental and calculated $2 \rightarrow 1$ transition probabilities as a function of the number of measurement pulses n. The transition probabilities for $n = 32$ and $n = 64$ are higher than the corresponding ones for the $1 \rightarrow 2$ transition because of an optical pumping effect discussed in the text.

TABLE I. Predicted and observed values of the $1 \rightarrow 2$ and $2 \rightarrow 1$ transition probabilities for different values of the number of measurement pulses n. The uncertainties of the observed transition probabilities are about 0.02. The second column shows the transition probabilities that result from a simplified calculation, in which the measurement pulses are assumed to have zero duration and in which optical pumping is neglected.

		$1 \rightarrow 2$ transition	
n	$\frac{1}{2}[1-\cos^n(\pi/n)]$	Predicted	Observed
1	1.0000	0.995	0.995
2	0.5000	0.497	0.500
4	0.3750	0.351	0.335
8	0.2346	0.201	0.194
16	0.1334	0.095	0.103
32	0.0716	0.034	0.013
64	0.0371	0.006	−0.006

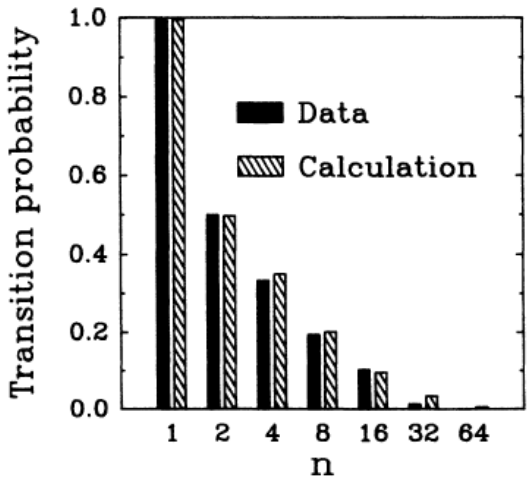

FIG. 3. Graph of the experimental and calculated $1 \rightarrow 2$ transition probabilities as a function of the number of measurement pulses n. The decrease of the transition probabilities with increasing n demonstrates the quantum Zeno effect.

How many photons need to be detected during the probe pulse to collapse the state?

How many photons need to be *emitted* during the probe pulse to collapse the state?

TABLE I. Predicted and observed values of the $1 \rightarrow 2$ and $2 \rightarrow 1$ transition probabilities for different values of the number of measurement pulses n. The uncertainties of the observed transition probabilities are about 0.02. The second column shows the transition probabilities that result from a simplified calculation, in which the measurement pulses are assumed to have zero duration and in which optical pumping is neglected.

n	$\frac{1}{2}[$	$2 \rightarrow 1$ transition	
		Predicted	Observed
1		0.999	0.998
2		0.501	0.496
4		0.365	0.363
8		0.217	0.209
16		0.118	0.106
32		0.073	0.061
64		0.080	0.075

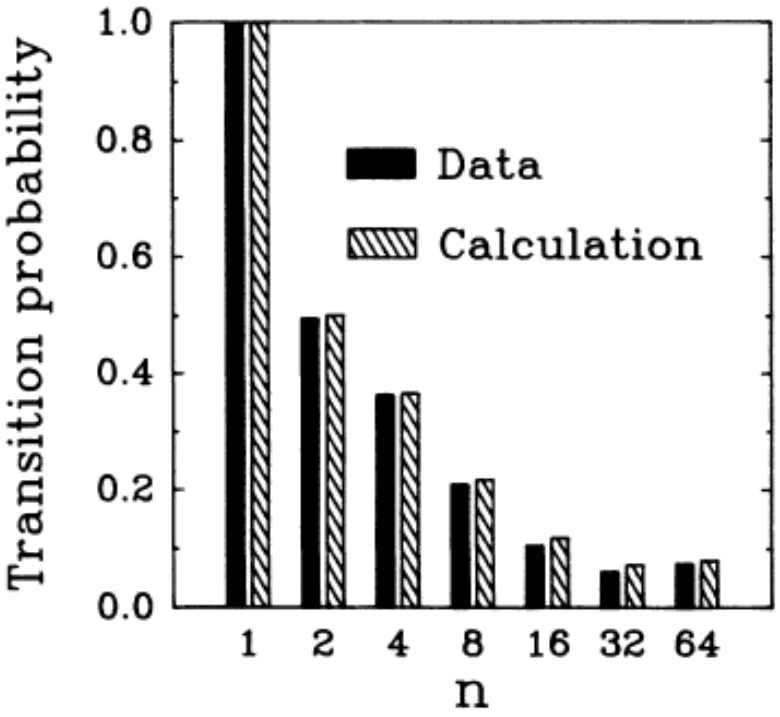

FIG. 4. Graph of the experimental and calculated $2 \rightarrow 1$ transition probabilities as a function of the number of measurement pulses n. The transition probabilities for $n = 32$ and $n = 64$ are higher than the corresponding ones for the $1 \rightarrow 2$ transition because of an optical pumping effect discussed in the text.

Asher Perez, Amer. Journ. Phys. **48** 931 (1980)

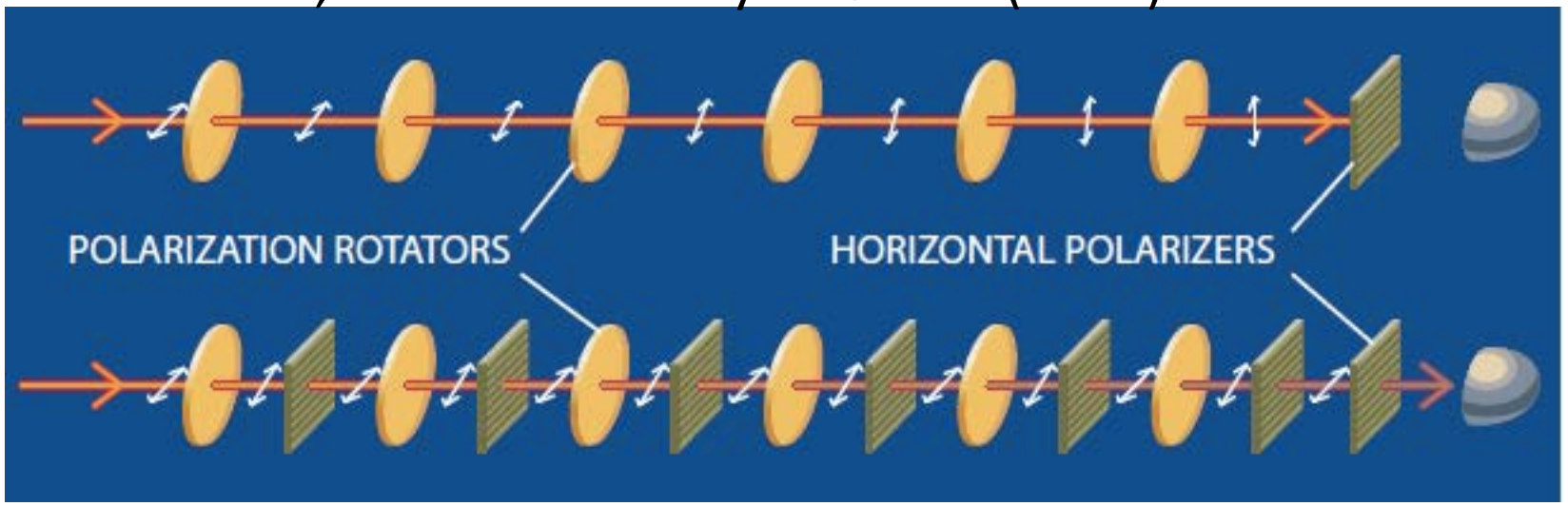

$$P_{trans} = \left[\cos^2\left(\frac{\pi}{2N}\right)\right]^N \xrightarrow[N\to\infty]{} 1$$

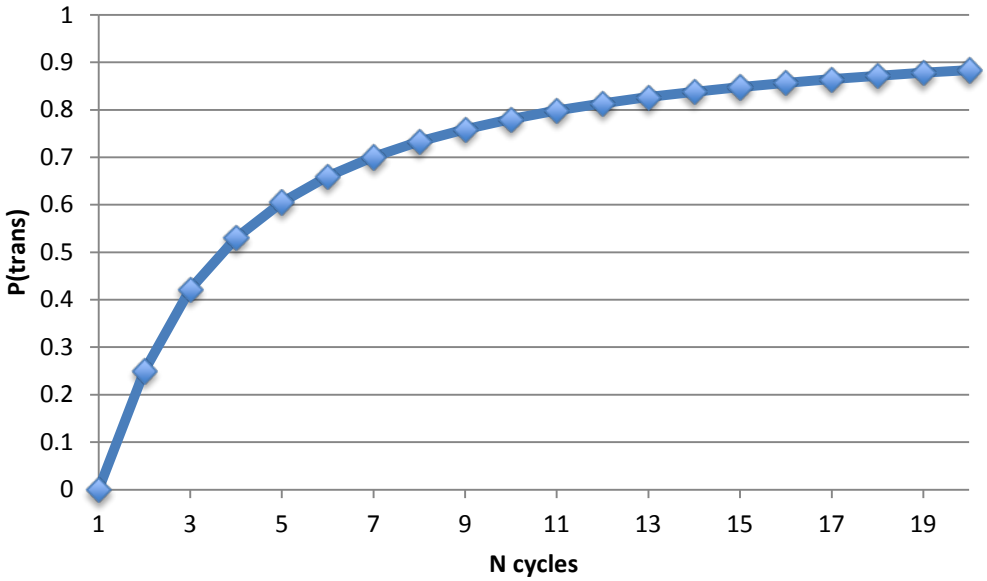

DEMO!

Q. Zeno with 'null measurements'

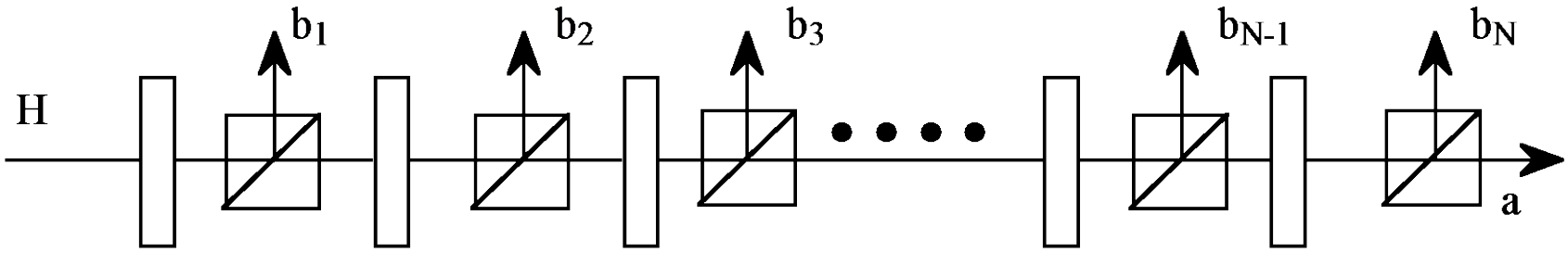

$$\cos^N x\left|H\right\rangle_a + \cos^{N-1} x \sin x\left|V\right\rangle_{bN} + \cos^{N-2} \sin x\left|V\right\rangle_{b(N-1)}$$

$$+ \ldots + \cos x \sin x\left|V\right\rangle_{b2} + \sin x\left|V\right\rangle_{b1}$$

Any detector 'click' certainly 'collapses' the wavefunction (if you believe in collapse). How does the wavefunction evolve?

It depends on which detectors are hit in what order.

E.g., photon amplitude hits D_{b1} first. If it *doesn't* fire, this (partially) collapses the wavefunction (last term disappears, renormalize the rest)

If photon amplitude then hits D_{b3}, then that detector's non-firing will eliminate that term in the state.

Quantum Interrogation

The problem…

Measure

-film

-absorber

-atom

without

-exposing

-heating

-exciting it

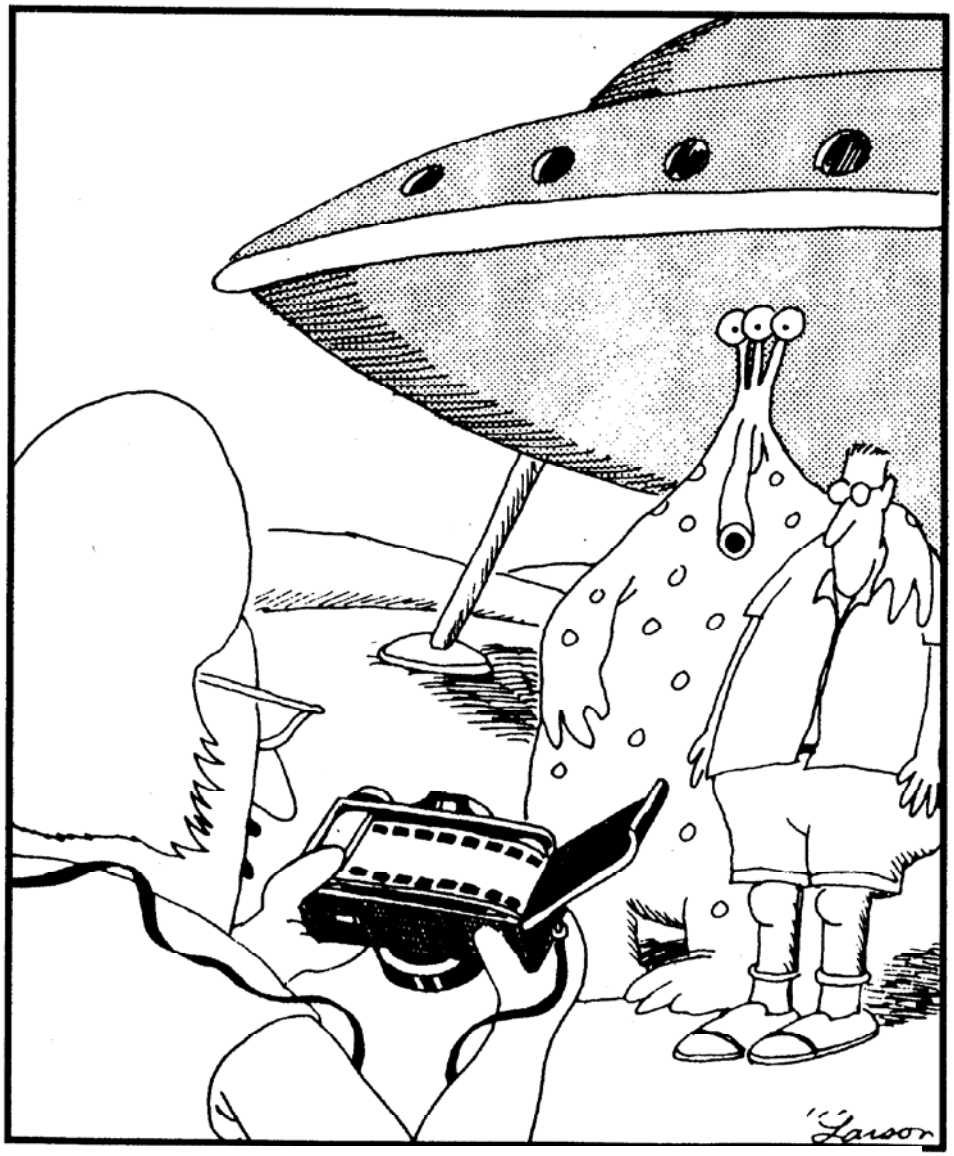

"Yes, yes, already, Warren! …

There *is* film in the camera!"

The solution… (Elitzur & Vaidman, 1993)

Use quantum "complementarity" -- dual wave-particle nature of quantum objects ("wavicles")

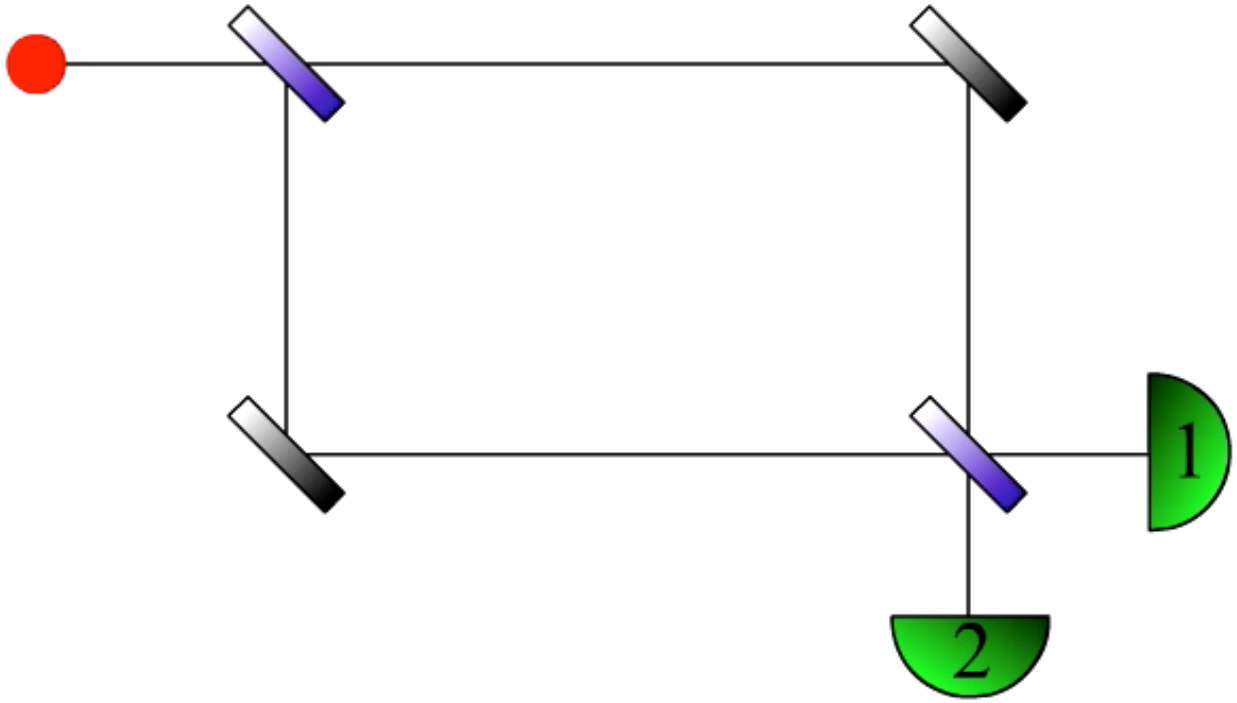

Single photon always shows up at D1
(complete destructive interference to D2)

Now place an absorbing object in one arm…

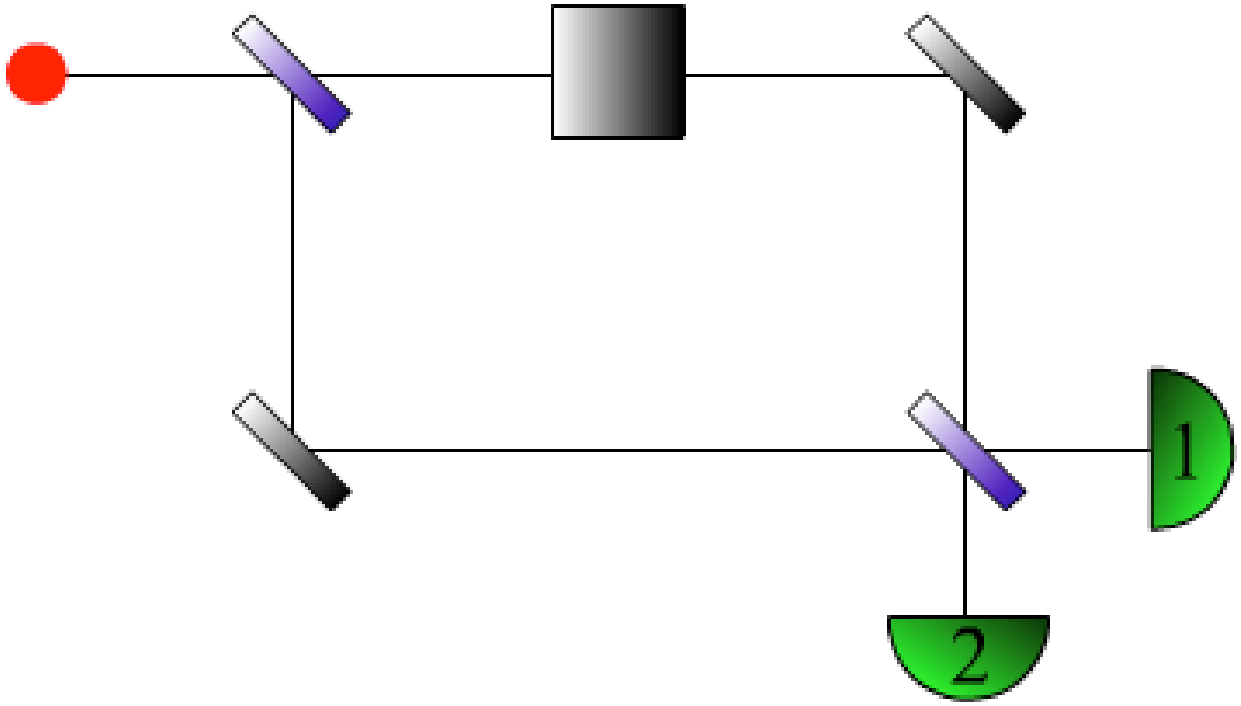

50% chance that photon is absorbed by object
50% chance it isn´t → 25% chance D2 fires →
"interaction-free measurement" of object

Quantum Interrogation

- Optimizing reflectivities → 50% efficiency
- By combining these techniques with the "quantum Zeno effect" (making repeated very weak interactions), the efficiency can in principle be pushed to 100%: no photons absorbed by the absorbing object!

  [85% demonstrated to date]
- Imaging semi-transparent objects does *not* readily yield a gray-scale

High-Efficiency Quantum Interrogation Measurements via the Quantum Zeno Effect

P. G. Kwiat,[1,*] A. G. White,[1] J. R. Mitchell,[1] O. Nairz,[2,†] G. Weihs,[2,†] H. Weinfurter,[2,‡] and A. Zeilinger[2,†]

[1]*Physics Division, P-23, Los Alamos National Laboratory, Los Alamos, New Mexico 87545*

[2]*Institute for Experimental Physics, University of Innsbruck, Innsbruck 6020, Austria*

(Received 16 June 1999)

The phenomenon of quantum interrogation allows one to optically detect the presence of an absorbing object, without the measuring light interacting with it. In an application of the quantum Zeno effect, the object inhibits the otherwise coherent evolution of the light, such that the probability that an interrogating photon is absorbed can in principle be arbitrarily small. We have implemented this technique, achieving efficiencies of up to 73%, and consequently exceeding the 50% theoretical maximum of the original "interaction-free" measurement proposal. We have also predicted and experimentally verified a previously unsuspected dependence on loss.

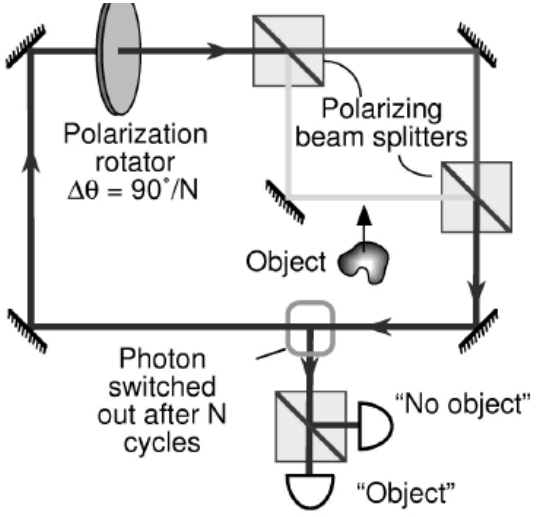

FIG. 1. Simple schematic of a hybrid scheme to allow high-efficiency quantum interrogation of the presence of an opaque object. With no object, the initial horizontal polarization of the interrogating photon is rotated stepwise to vertical. The presence of an object in the **V** arm inhibits this evolution via the optical quantum Zeno effect [9], so that the final polarization after N cycles unambiguously indicates the presence or absence of the object: **V** polarization → no object; **H** polarization → object.

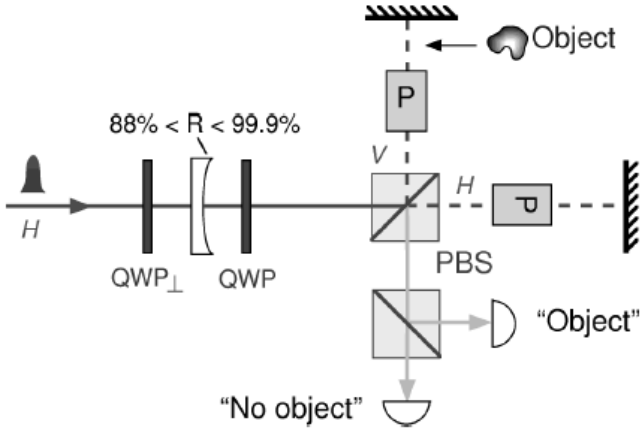

FIG. 2. Experimental system to demonstrate high-efficiency quantum interrogation. Photons from a pulsed laser at 670 nm are coupled into the recycling system via a high-reflectivity recycling mirror (initially flat, later curved; see Fig. 3). A double pass through the quarter wave plate (QWP) served to rotate the polarization by a fixed amount during each cycle; an extra wave plate ($QWP_\perp$) in the entrance beam was used to compensate for the initial pass. On each cycle the photon passed through a polarization interferometer [with a polarizing beam splitter (PBS)]; to fine-tune the interferometer phase, one mirror was mounted on a piezoelectric "bimorph." The Pockels cells (P) were used to switch the photons out after a desired number of cycles—a ~3 kV pulse was applied, which after the double pass rotated the polarization of the photon by 90°, so that it exited via the other port of the PBS. The exiting photon was then analyzed by the adjustable polarizer and single-photon detector [EG&G No. SPCM-AQ-141, preceded by an interference filter (10 nm FWHM, centered at 670 nm) to reduce background]. The final polarization of the detected photon indicates the presence (**V** polarized) or absence (**H** polarized) of an object in the reflected arm of the interferometer. (Not shown: an active feedback helium neon laser which ran below the plane of the 670 nm light, to stabilize the interferometer.)

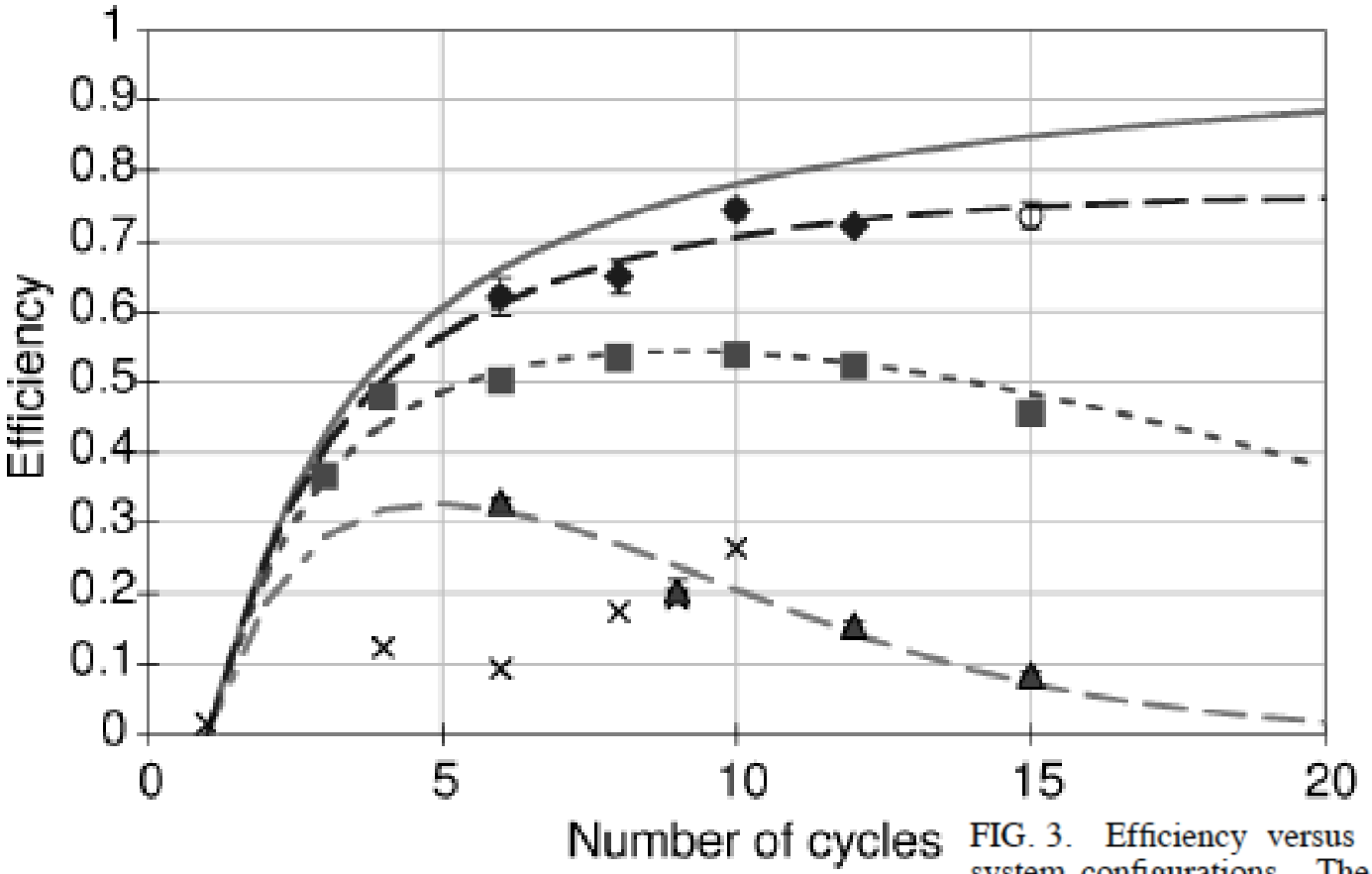

FIG. 3. Efficiency versus number of cycles N for several system configurations. The curves are theoretical predictions based on the measured losses for each configuration. The triangles and the dotted-dashed curve correspond to a lossy nonswitching system in which the photons experienced 8% loss/cycle due to the input coupler, and leaked out through a flat 88% reflective output coupler. The squares and dotted curve correspond to the system in Fig. 2, with a somewhat lossy Pockels cell in the no-object arm ($T = 95.1\%$) and a flat recycling mirror ($R = 96.2\%$). The diamonds and the dashed curve correspond to a better Pockels cell ($T = 97.7\%$) and a curved recycling mirror ($R = 97.4\%$), and the circle corresponds to a higher reflectivity ($R = 99.4\%$) curved mirror. The solid curve is the prediction for a lossless system. Several representative measurements of the noise in our quantum interrogation process are also shown (crosses).

Inhibited Spontaneous Emission by a Rydberg Atom

Randall G. Hulet,[a] Eric S. Hilfer, and Daniel Kleppner

Research Laboratory of Electronics and Department of Physics, Massachusetts Institute of Technology, Cambridge, Massachusetts 02139

(Received 29 July 1985)

Spontaneous radiation by an atom in a Rydberg state has been inhibited by use of parallel conducting planes to eliminate the vacuum modes at the transition frequency. Spontaneous emission is observed to "turn off" abruptly at the cutoff frequency of the waveguidelike structure and the natural lifetime is measured to increase by a factor of at least 20.

$$(n = 22, |m| = 21) \rightarrow (n = 21, |m| = 20)$$

$$\lambda = 0.45 \text{ mm}$$

The experiment was performed with a thermal atomic beam of cesium. The beam passes sequentially through three regions: a production region where the atoms are transferred to the circular state, a drift region inside the parallel-plate cavity with a mean transit time approximately equal to the free-space radiation lifetime, and finally the detector where the arrival times of the $n = 22$ atoms are recorded. Spontaneous emission changes the shape of the time-of-flight curve from the usual Maxwellian form for an atomic beam.[8] When the emission is inhibited, the curve reverts to its usual form and there is a dramatic increase in the overall transmission. To switch from enhanced to in-

The cavity consists of two gold-plated aluminum plates, 6.4 cm wide $\times$ 12.7 cm long, that are separated by six disk-shaped quartz spacers. The spacer thickness, 230.1 μm, is $1.02(\lambda_0/2)$, where λ_0 is the transition wavelength in zero field. The circular states have

Inhibited emission

$$\frac{dN}{dt} = \frac{N_0}{t_0}\left(\frac{t_0}{t}\right)^5 e^{-(t_0/t)^2} e^{-\Gamma t}.$$

Γ is the radiative decay rate. $t_0 = L/\alpha$, where L is the time-of-flight distance and $\alpha = (2kT/M)^{1/2}$ is the most probable speed in the source. N_0 is a normalization

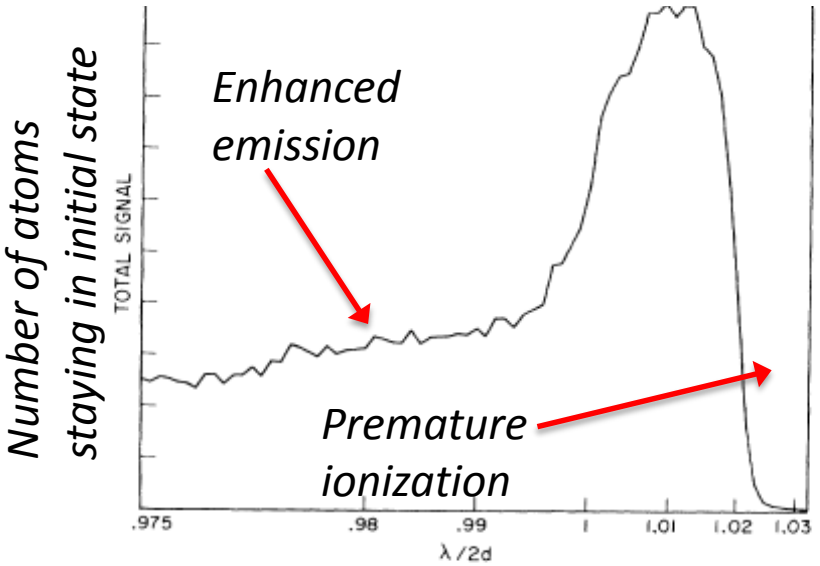

FIG. 4. Total transmission signal for $\lambda/2d$ near the cutoff region. (λ is altered by application of an electric field, which increases from 0 to 3.1 kV/cm for the data shown.) The sharp increase in transmission at $\lambda/2d = 1$ is due to the inhibition of spontaneous emission; the decrease for $\lambda/2d > 1.015$ is due to field ionization between the cavity plates.

When might we want to increase the rate of emission?

On-Demand Single Photons with High Extraction Efficiency and Near-Unity Indistinguishability from a Resonantly Driven Quantum Dot in a Micropillar

Xing Ding,[1,2,3] Yu He,[1,2,3] Z.-C. Duan,[1,2,3] Niels Gregersen,[4] M.-C. Chen,[1,2,3] S. Unsleber,[5] S. Maier,[5] Christian Schneider,[5] Martin Kamp,[5] Sven Höfling,[1,5,6] Chao-Yang Lu,[1,2,3,*] and Jian-Wei Pan[1,2,3,†]

Scalable photonic quantum technologies require on-demand single-photon sources with *simultaneously* high levels of purity, indistinguishability, and efficiency. These key features, however, have only been demonstrated separately in previous experiments. Here, by *s*-shell pulsed resonant excitation of a Purcell-enhanced quantum dot-micropillar system, we deterministically generate resonance fluorescence single photons which, at π pulse excitation, have an extraction efficiency of 66%, single-photon purity of 99.1%, and photon indistinguishability of 98.5%. Such a single-photon source for the first time combines the features of high efficiency and near-perfect levels of purity and indistinguishabilty, and thus opens the way to multiphoton experiments with semiconductor quantum dots.

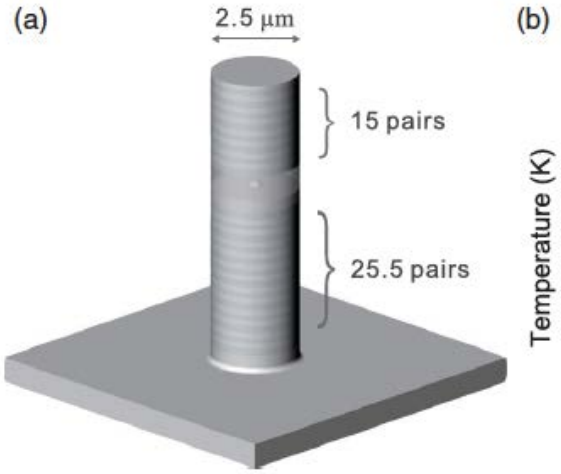

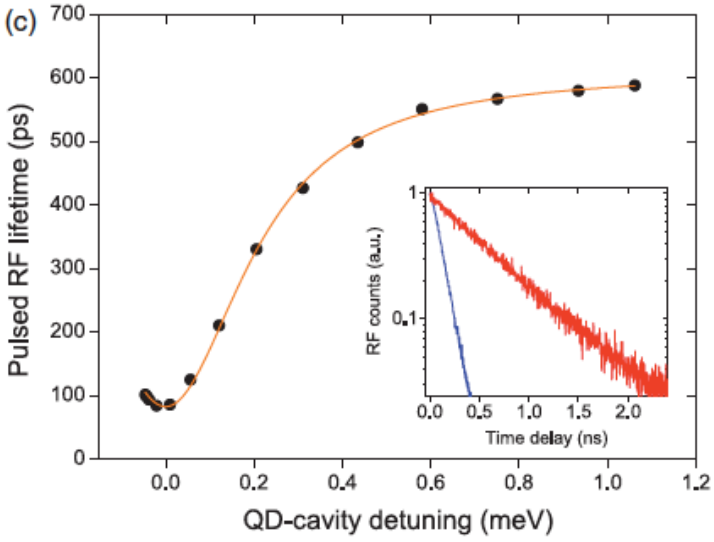

Achieved Q ~6100

→ $F_{purcell} = 6.3(4)$

→ decay reduced from 590ps to 84 ps

Light interference from single atoms and their mirror images

J. Eschner*†, Ch. Raab*†, F. Schmidt-Kaler† & R. Blatt†

NATURE | VOL 413 | 4 OCTOBER 2001 | www.nature.com

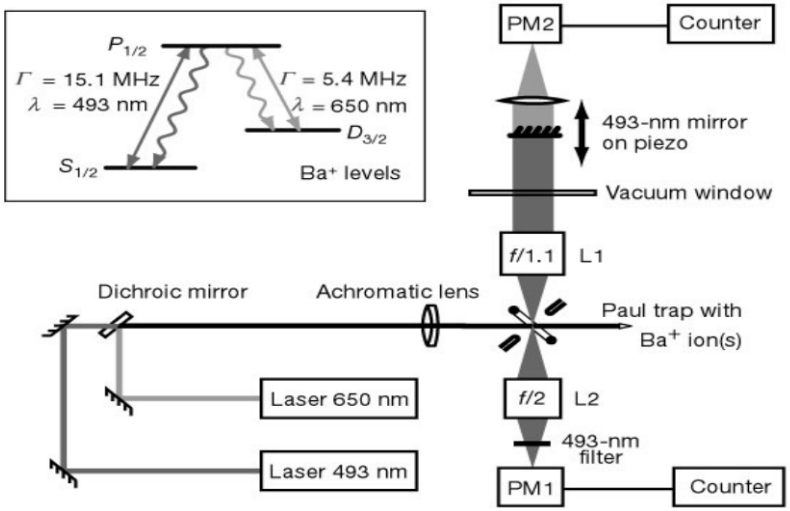

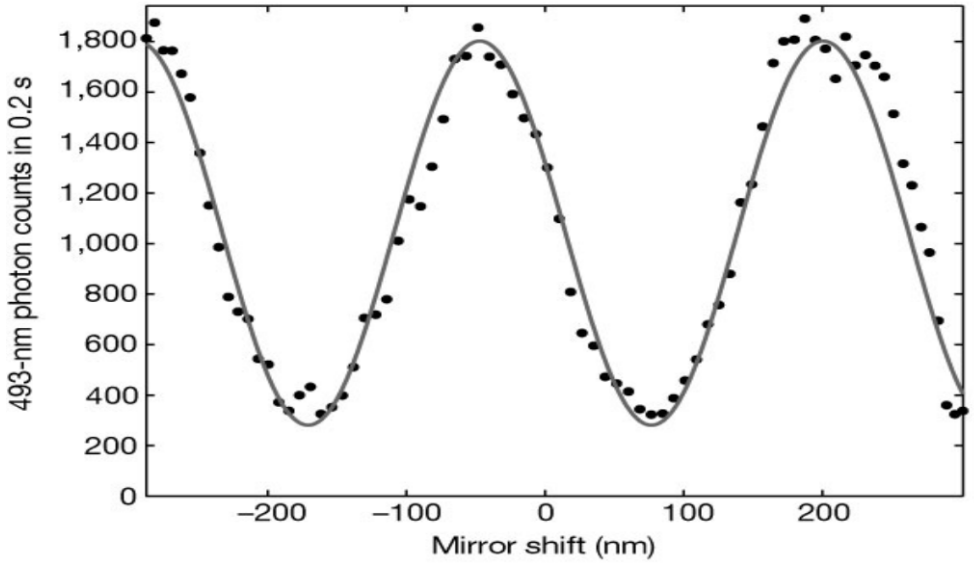

Acceleration of quantum decay processes by frequent observations

A. G. Kofman & G. Kurizki

NATURE | VOL 405 | 1 JUNE 2000 | www.nature.com

Department of Chemical Physics, The Weizmann Institute of Science, Rehovot 76100, Israel

In theory, the decay of any unstable quantum state can be inhibited by sufficiently frequent measurements—the quantum Zeno effect[1–10]. Although this prediction has been tested only for transitions between two coupled, essentially stable states[5–8], the quantum Zeno effect is thought to be a general feature of quantum mechanics, applicable to radioactive[3] or radiative decay processes[6,9]. This generality arises from the assumption that, in principle, successive observations can be made at time intervals too short for the system to change appreciably[1–4]. Here we show not only that the quantum Zeno effect is fundamentally unattainable in radiative or radioactive decay (because the required measurement rates would cause the system to disintegrate), but also that these processes may be accelerated by frequent measurements. We find that the modification of the decay process is determined by the energy spread incurred by the measurements (as a result of the time–energy uncertainty relation), and the distribution of states to which the decaying state is coupled. Whereas the inhibitory quantum Zeno effect may be feasible in a limited class of systems, the opposite effect—accelerated decay—appears to be much more ubiquitous.

Observation of the Quantum Zeno and Anti-Zeno Effects in an Unstable System

M. C. Fischer, B. Gutiérrez-Medina, and M. G. Raizen

Department of Physics, The University of Texas at Austin, Austin, Texas 78712-1081

(Received 30 March 2001; published 10 July 2001)

We report the first observation of the quantum Zeno and anti-Zeno effects in an unstable system. Cold sodium atoms are trapped in a far-detuned standing wave of light that is accelerated for a controlled duration. For a large acceleration the atoms can escape the trapping potential via tunneling. Initially the number of trapped atoms shows strong nonexponential decay features, evolving into the characteristic exponential decay behavior. We repeatedly measure the number of atoms remaining trapped during the initial period of nonexponential decay. Depending on the frequency of measurements we observe a decay that is suppressed or enhanced as compared to the unperturbed system.

Our experiment consists of ultracold sodium atoms in an accelerated standing wave of light which creates an optical potential of the form $V_0 \cos[2k_L x - k_L a t^2]$, where V_0 is the amplitude of the potential, k_L is the wave number of the light forming the potential, x is the position in the laboratory frame, a is the acceleration, and t is time. Transments on the system decay rate. The quantity to be measured was the number of atoms remaining trapped in the potential during the tunneling segment. This measurement could be realized by suddenly interrupting the tunneling duration by a period of reduced acceleration a_{interr}, as indicated in Fig. 2(a). During this interruption, tunneling was negligible and the atoms were therefore transported to a higher velocity without being lost out of the well. This separation in velocity space enabled us to distinguish the remaining atoms from the ones having tunneled out up to the point of interruption, as can be seen in Fig. 2(b). By switching the acceleration back to a_{tunnel} the system was then returned to its unstable state. The measurement of the number of atoms defined a new initial state, with the remaining number of atoms as the initial condition. The system must therefore start the evolution again with the same nonexponential decay features. The requirements for this

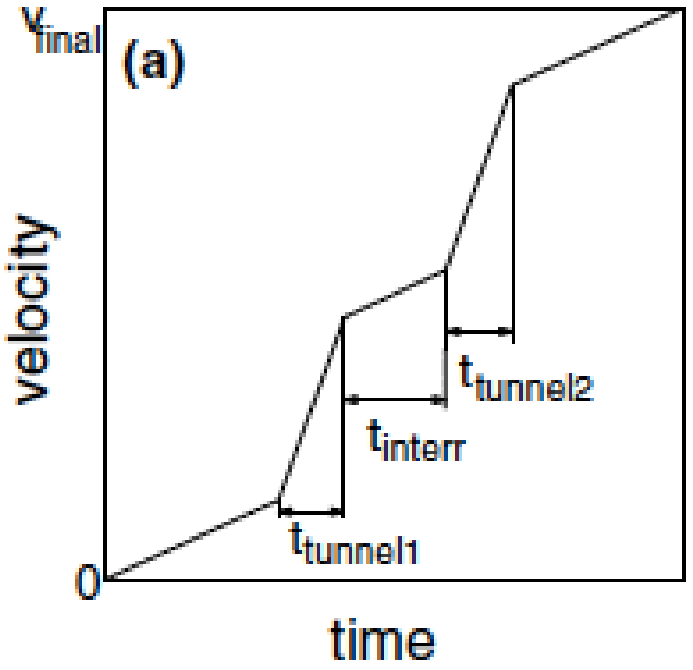

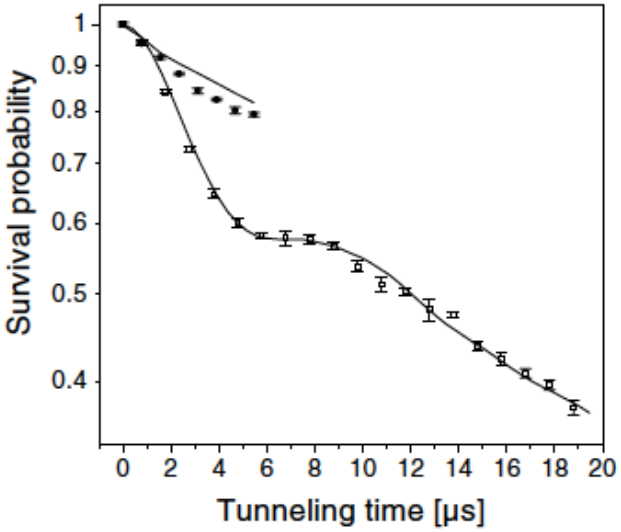

FIG. 3. Probability of survival in the accelerated potential as a function of duration of the tunneling acceleration. The hollow squares show the noninterrupted sequence, and the solid circles show the sequence with interruptions of 50 μs duration every 1 μs. The error bars denote the error of the mean. The data have been normalized to unity at $t_{\text{tunnel}} = 0$ in order to compare with the simulations. The solid lines are quantum mechanical simulations of the experimental sequence with no adjustable parameters. For these data the parameters were $a_{\text{tunnel}} = 15\,000$ m/s^2, $a_{\text{interr}} = 2000$ m/s^2, $t_{\text{interr}} = 50$ μs, and $V_0/h = 91$ kHz, where h is Planck's constant.

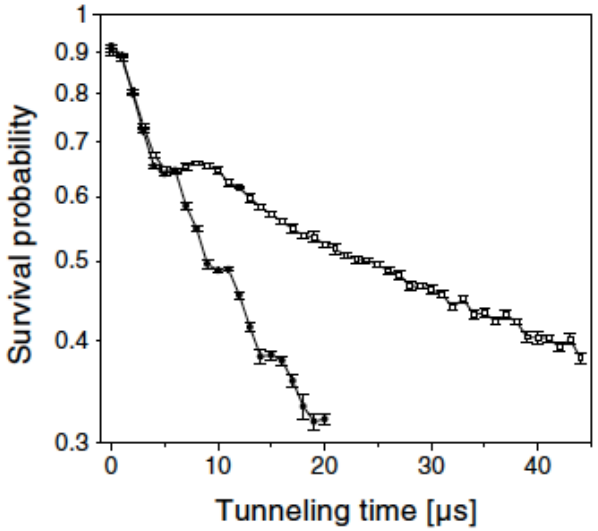

FIG. 4. Survival probability as a function of duration of the tunneling acceleration. The hollow squares show the noninterrupted sequence, and the solid circles show the sequence with interruptions of 40 μs duration every 5 μs. The error bars denote the error of the mean. The experimental data points have been connected by solid lines for clarity. For these data the parameters were: $a_{\text{tunnel}} = 15\,000$ m/s^2, $a_{\text{interr}} = 2800$ m/s^2, $t_{\text{interr}} = 40$ μs, and $V_0/h = 116$ kHz.

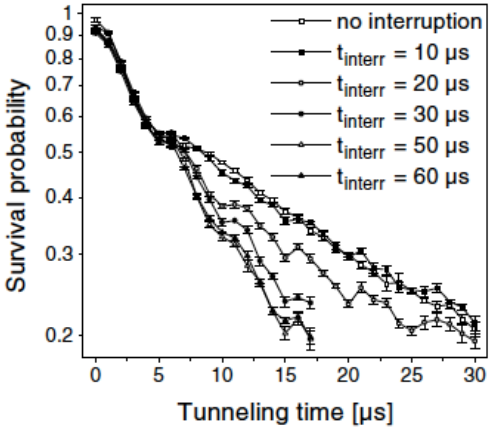

FIG. 5. Survival probability as a function of duration of the tunneling acceleration. The hollow squares show the noninterrupted sequence, and the other symbols indicate the sequence with a finite interruption duration after every 5 μs of tunneling. The error bars denote the error of the mean. A further than indicated increase of the interruption duration does not result in a further change of the decay behavior. The experimental data points have been connected by solid lines for clarity. For these data the parameters were $a_{\text{tunnel}} = 15\,000$ m/s^2, $a_{\text{interr}} = 2000$ m/s^2, and $V_0/h = 91$ kHz.

Quantum anti-Zeno effect without wave function reduction

Qing Ai[1,2], Dazhi Xu[1,2], Su Yi[1,2], A. G. Kofman[1,3], C. P. Sun[1,4] & Franco Nori[1,3,5]

[1]CEMS, RIKEN, Saitama 351-0198, Japan, [2]Institute of Theoretical Physics, Chinese Academy of Sciences, Beijing 100190, China, [3]Physics Department, The University of Michigan, Ann Arbor, Michigan 48109-1040, USA, [4]Beijing Computational Science Research Center, Beijing 100084, China, [5]Department of Physics, Korea University, Seoul 136-713, Korea.

We study the measurement-induced enhancement of the spontaneous decay for a two-level subsystem, where measurements are treated as couplings between the excited state and an auxiliary state rather than the von Neumann's wave function reduction. The photon radiated in a fast decay of the atom, from the auxiliary state to the excited state, triggers a quasi-measurement, as opposed to a projection measurement. Our use of the term "quasi-measurement" refers to a "coupling-based measurement". Such frequent quasi-measurements result in an exponential decay of the survival probability of atomic initial state with a photon emission following each quasi-measurement. Our calculations show that the effective decay rate is of the same form as the one based on projection measurements. The survival probability of the atomic initial state obtained by tracing over all the photon states is equivalent to that of the atomic initial state with a photon emission following each quasi-measurement.

SCIENTIFIC REPORTS | 3 : 1752 | DOI: 10.1038/srep01752 (2013)

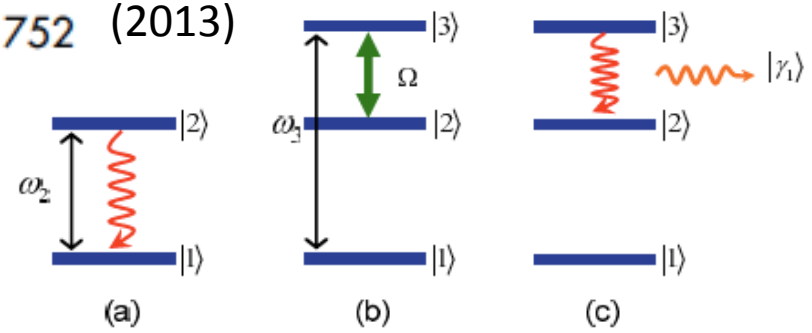

Figure 1 | Energy level diagram for the three processes considered here: (a) the spontaneous decay from the excited state $|2\rangle$ to the ground state $|1\rangle$, (b) a coherent transition with Rabi frequency Ω between $|2\rangle$ and the auxiliary state $|3\rangle$ by laser pumping, and (c) a fast spontaneous decay from $|3\rangle$ to $|2\rangle$ with a photon emitted in $|\gamma_1\rangle$. Here, the eigenenergies for the excited state and the auxiliary state are ω_2 and ω_3, respectively.

PHYSICAL REVIEW E **80**, 056115 (2009)

Quantum Zeno effect explains magnetic-sensitive radical-ion-pair reactions

I. K. Kominis*
Department of Physics, University of Crete, Heraklion 71103, Greece
and Institute of Electronic Structure & Laser, Foundation for Research and Technology, Heraklion 71110, Gr
(Received 19 February 2009; revised manuscript received 13 July 2009; published 24 November 2009)

Chemical reactions involving radical-ion pairs are ubiquitous in biology, since not only are they at the bas of the photosynthetic reaction chain, but are also assumed to underlie the biochemical magnetic compass us by avian species for navigation. Recent experiments with magnetic-sensitive radical-ion-pair reactions pr vided strong evidence for the radical-ion-pair magnetoreception mechanism, verifying the expected magne sensitivities and chemical product yield changes. It is here shown that the theoretical description of radic ion-pair reactions used since the 70s cannot explain the observed data, because it is based on phenomenologic equations masking quantum coherence effects. The fundamental density-matrix equation derived here fro basic quantum measurement theory considerations naturally incorporates the quantum Zeno effect and readi explains recent experimental observations on low- and high magnetic-field radical-ion-pair reactions.

The avian magnetic field detection is governed by the interplay between magnetic interactions of the radicals unpaired electrons and the radicals recombination dynamics. Critical to this mechanism is the long lifetime of the radical-pair spin coherence, so that the weak geomagnetic field will have a chance to signal its presence. It is here shown that a fundamental quantum phenomenon, the quantum Zeno effect, is at the basis of the radical-ion-pair magnetoreception mechanism. The quantum Zeno effect naturally leads to long spin coherence lifetimes, without any constraints on the systems physical parameters, ensuring the robustness of this sensory mechanism.